

Structure-Based Virtual Screening Approach for Discovery of Covalently Bound Ligands

Dora Toledo Warshaviak,^{†,§} Gali Golan,^{‡,§} Kenneth W. Borrelli,[†] Kai Zhu,[†] and Ori Kalid^{*,‡}

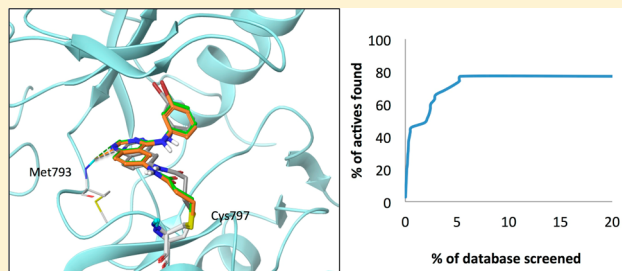
[†]Schrödinger Inc., 120 West 45th Street, New York, New York 10036, United States

[‡]Karyopharm Therapeutics, 2 Mercer Road, Natick, Massachusetts 01760, United States

Supporting Information

ABSTRACT: We present a fast and effective covalent docking approach suitable for large-scale virtual screening (VS). We applied this method to four targets (HCV NS3 protease, Cathepsin K, EGFR, and XPO1) with known crystal structures and known covalent inhibitors. We implemented a customized “VS mode” of the Schrödinger Covalent Docking algorithm (CovDock), which we refer to as CovDock-VS. Known actives and target-specific sets of decoys were docked to selected X-ray structures, and poses were filtered based on noncovalent protein–ligand interactions known to be important for activity.

We were able to retrieve 71%, 72%, and 77% of the known actives for Cathepsin K, HCV NS3 protease, and EGFR within 5% of the decoy library, respectively. With the more challenging XPO1 target, where no specific interactions with the protein could be used for postprocessing of the docking results, we were able to retrieve 95% of the actives within 30% of the decoy library and achieved an early enrichment factor (EF1%) of 33. The poses of the known actives bound to existing crystal structures of 4 targets were predicted with an average RMSD of 1.9 Å. To the best of our knowledge, CovDock-VS is the first fully automated tool for efficient virtual screening of covalent inhibitors. Importantly, CovDock-VS can handle multiple chemical reactions within the same library, only requiring a generic SMARTS-based predefinition of the reaction. CovDock-VS provides a fast and accurate way of differentiating actives from decoys without significantly deteriorating the accuracy of the predicted poses for covalent protein–ligand complexes. Therefore, we propose CovDock-VS as an efficient structure-based virtual screening method for discovery of novel and diverse covalent ligands.



INTRODUCTION

In recent years, there has been a growing interest in the design of drugs forming a covalent bond with the target protein, with nearly 30% of the marketed drugs targeting enzymes known to act by covalent inhibition.¹ Covalent interaction with the target protein has the benefit of prolonged duration of the biological effect and potential for improved selectivity. Examples of proteins that have been targeted by covalent drugs include serine penicillin-binding proteins (PBPs) which bind to β -lactams and β -lactone antibiotics, cysteine proteases such as Cathepsin B, K, and S, which are covalently modified by vinyl sulfones, epoxides, isothiazolones, and ketoamides, as well as other chemical groups, and hepatitis C virus (HCV) protease, which covalently binds the ketoamide groups of boceprevir and telaprevir.

The concept of irreversible drug design has been a subject of debate. The reluctant attitude toward covalent drugs is mostly due to safety concerns, related to nonspecific reactivity. Nonspecific reactivity may either be due to off-target binding or to the *in vivo* production of reactive metabolites that may lead to adverse effects such as tissue injury and immune response.² A possible approach to lower the risk for off-target binding is the rational design of highly selective and specific covalent compounds, designed to react with a noncatalytic,

poorly conserved nucleophilic amino acid in the target protein. The reactive groups used in this case are weaker electrophiles, reducing the risk of broad range nonspecific reactivity. An example of a recently reported class of rationally designed covalent drugs is SINE (Selective Inhibitors of Nuclear Export), which covalently inhibit the major nuclear export protein XPO1 (also referred to as chromosome region maintenance 1 or CRM1).³ The most advanced SINE, Selinexor (KPT-330), is now in phase 1/2 clinical trials for a range of hematological and solid malignancies (NCT01607905, NCT01607892, NCT01986348, and NCT02025985). SINE compounds were shown to bind covalently to Cys528 of XPO1. Another example is Afatinib, targeting the noncatalytic cysteine 797 of the epidermal growth factor receptor (EGFR) tyrosine kinase, which was recently approved as first-line treatment for metastatic nonsmall-cell lung cancer (NSCLC) patients with EGFR mutations.

The covalent bond between the reactive group of the drug and the targeted protein residue can be either reversible or irreversible. Reversible covalent drugs may benefit from the strength of the covalent interaction while relieving some of the

Received: March 18, 2014



potential liabilities due to long-term inhibition of off-target proteins. Recent advances in the design of reversible covalent drugs include kinase inhibitors with cyanoacrylamide and cyanoacrylate warheads replacing acrylamide/acrylate groups of irreversible covalent compounds. Compounds containing doubly activated inhibitors were shown to fully dissociate with a time scale of several hours, while a similar fluoromethylketone inhibitor behaved as fully irreversible binder.⁴ With the growing interest in covalent drug discovery, there is a clear need for a technology that could efficiently and effectively support structure-based virtual screening (SBVS) of covalent drugs. This is not available in the most commonly used docking tools for structure-based screening, e.g. Glide,^{5,6} GOLD,^{7,8} AutoDock,⁹ and FlexX,¹⁰ which are designed to predict noncovalent protein–ligand interactions.

Recently, several new covalent docking algorithms were introduced into some of the commercial docking tools, resulting in successful prediction of the binding poses relative to corresponding crystal structures.^{11,12} Generally, implementation of a covalent docking feature requires manual definition of the reactive atoms and reaction type as well as manual preparation of the ligand and protein structure files, leading to difficulties in up-scaling the process for screening purposes. CovalentDock,¹² which can be implemented into other docking suites, aims to address this problem by automatic preparation of ligand files but is limited in reaction types and protein rigidity. Notably, subject to these limitations, covalent docking with GOLD has successfully been used for small scale (1247 compounds) virtual screening.¹³

In order to facilitate rapid structure-based discovery of new and diverse covalent drugs, employing covalent docking tools should become a more automated straightforward task. First and foremost this would require automatic detection of diverse reactive groups within a single screening library and removal of all need for manual modification of protein or ligand structure files. In addition, reasonable execution time is necessary, and a generalized scoring function suitable for the comparison and relative ranking of different molecules is required. To the best of our knowledge, none of the existing software tools properly addresses all of these requirements, and thus in our view none provide an adequate solution for SBVS for covalent drugs.

Recently, a new covalent docking program (CovDock) was developed by Schrödinger.¹⁴ While CovDock yields good accuracy in binding mode prediction and has automatic detection of reactive atoms using SMARTS patterns, it does not facilitate SBVS due to calculation length. Herein, we report the development of a modified version, CovDock-VS (CovDock Virtual Screening), specifically tailored to address all of the SBVS requirements detailed above. CovDock-VS was validated by retrospective SBVS performed on four highly diverse drug targets. Our results demonstrate that CovDock-VS is a straightforward and efficient method that can be applied successfully in screening campaigns for covalent inhibitors.

METHODS

CovDock-VS. In this work, we describe a modified version of the Covalent Docking (CovDock) workflow implemented in Schrödinger Suite,¹⁴ which we refer to as the Virtual Screening (VS) mode. We made changes to the default method, which is referred to as the Lead Optimization (CovDock-LO) mode, so that it is fast enough to be used for SBVS (Workflow summarized in Figure 1). The Schrödinger CovDock algorithm uses both Glide and Prime.^{5,6,15} It is developed to mimic the

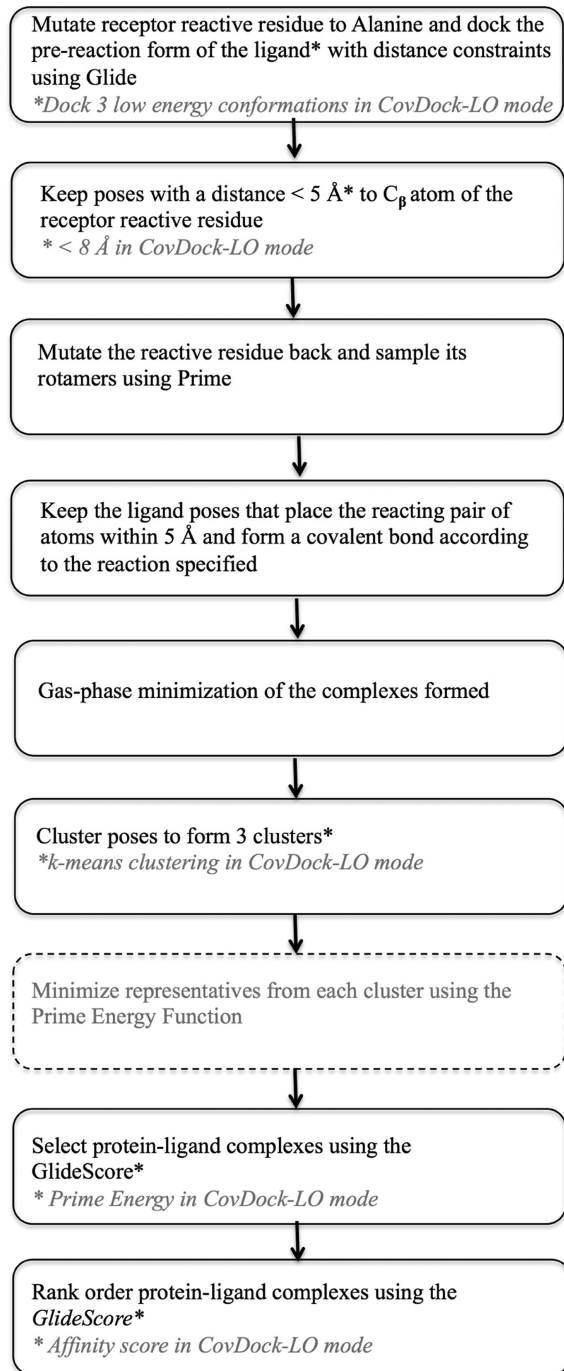


Figure 1. CovDock-VS workflow. The grayed out text and stages show the steps that were omitted or modified in CovDock-LO mode for virtual screening purposes.

covalent ligand binding by first positioning the prereaction form of the ligand in the binding site close to the receptor reactive residue using Glide docking with positional constraints and only then generating the covalent attachment. In the prereaction docking step, the reactive residue is mutated to alanine to enable a closer approach by the reactive group of the ligand. A maximum of 10 poses per ligand are kept and subject to postdocking minimization. All poses within 2.5 GlideScore units of the minimum are retained, and poses with a distance greater than 5 Å to C_β atom of the receptor reactive residue are rejected. The default CovDock protocol involves sampling

ligand conformations using ConfGen¹⁶ prior to docking. We skipped this step in CovDock-VS for the sake of reducing the computation time. In the following steps, the reactive residue is mutated back, and its rotamers are sampled using the Prime VSGB2.0 energy model¹⁵ with the OPLS2005 force field.^{17,18} Ligand poses that place the reacting pair of atoms within 5 Å are kept, and a covalent bond is formed according to the reaction specified accompanied by any bond order changes and hydrogen abstractions/additions. The two reactions studied in this work (Michael addition and Nucleophilic addition to α -ketoamides) are shown in Figure 2. The reactive group on the

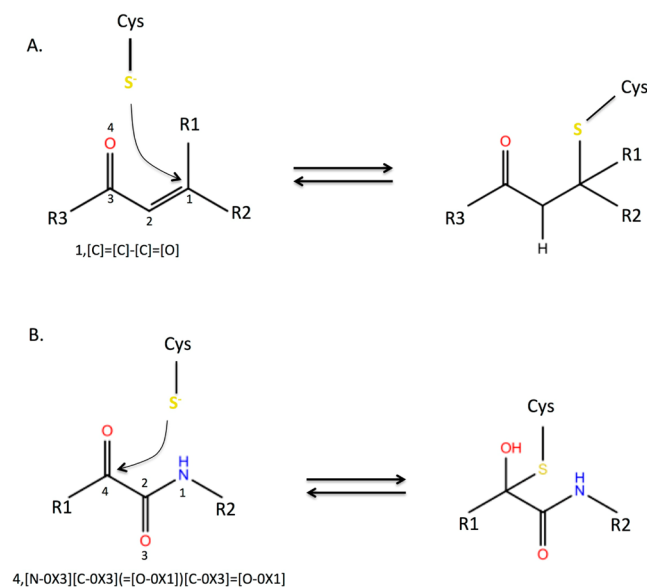


Figure 2. Examples of covalent binding reactions used in the virtual screening study. The SMARTS patterns defining the reactive groups in the ligands are shown below the reactants. The numbering of reactant atoms correspond to the SMARTS blocks. A. Michael addition reaction. The reactive atom is specified by the index number 1, corresponding to the 1st block in the SMARTS pattern; B. Nucleophilic addition to α -ketoamides. The reactive atom is specified by the index number 4, corresponding to the 4th block in the SMARTS pattern.

ligand is specified with a SMARTS pattern. Many common reactions (i.e., Michael addition, epoxide opening, Nucleophilic addition, etc.) are predefined to recognize the ligand reactive group with the encoded SMARTS pattern and to perform the postreaction changes in hybridization of the ligand. However, it is possible to define a custom SMARTS pattern for the predefined reaction, which is more specific, as well as add a new custom reaction. In the case of Nucleophilic addition reaction to α -ketoamides, we defined the reaction using the Maestro format SMARTS pattern 4,[N-0X3][C-0X3](=[O-0X1])[C-0X3]=[O-0X1] to identify the α -ketoamide group. A reactive atom is specified by the index number 4, corresponding to the fourth block in the SMARTS pattern (Figure 2).

The covalent complexes formed are minimized in gas-phase and then clustered by their Cartesian coordinates; three clusters are formed to remove duplicates and reduce the number of complexes that are carried forward to postprocessing. The CovDock algorithm in the default mode¹⁴ uses k-means clustering and generates a large number of clusters (around 20 clusters) for further refinement using the Prime Energy Function.¹⁵ We found that using three clusters and limiting

optimization to a gas-phase optimization of the ligand and the covalently bound protein residue sped up the calculations dramatically while still yielding high quality poses. We used the initial GlideScore^{5,6} to select protein–ligand complexes and for rank ordering them instead of using the affinity score described by Zhu et al.¹⁴ In addition, we chose to output the three best poses for the complexes based on their initial GlideScore. When relevant (for HCV NS3 protease, Cathepsin K, and EGFR), these poses were filtered to remove any poses that did not contain H-bond interaction between known actives and the protein as described in the literature.^{19–21} We then analyzed the best pose per ligand that satisfied the filters.

Ligand and Protein Preparation. When running enrichment studies it is important to use a decoy library with similar physicochemical properties (molecular weight, H-bond donor, H-bond acceptor, number of rotatable bonds, ring count, and AlogP) to the known actives in order to avoid false enrichment rates. In our case, the decoys also had to include the same chemical warheads as the actives (Figure S2). In the case of Cathepsin K and HCV NS3 protease, a search for peptidomimetic decoys with α -ketoamide reactive groups led to only 54 molecules (all from the ChemDiv collection). Therefore, we used the BREED²² algorithm to generate virtual decoys. Two generations of molecular breeding were performed, and the resulting molecules were filtered using molecular property ranges derived from properties of the active molecules (Figure S1). In addition, only molecules with a single α -ketoamide group were kept. The filtering resulted in 1562 virtual decoy compounds (Figure S1).

For EGFR and XPO1, decoys were selected from a virtual library of commercially available compounds from various vendors. The compounds were first filtered according to the warheads found in the known inhibitors of EGFR and XPO1 and then further filtered according to drug-like properties and parameters of the known inhibitors (Figure S1). Additionally, large ring systems and spiro structures were removed using combination of the properties such as chirality count and ring fusion density.

Known active ligands were selected from the literature for each target (Table 1, Figure S2). Both the active ligands and

Table 1. Number of Known Actives and Decoys Used in Virtual Screening

	number of known actives	number of decoys
HCV NS3 Protease	25 ^a	1562
Cathepsin K	21 ^b	1562
EGFR	34 ^c	5000
XPO1	21 ^d	5000

^aPotency range (2–4300 nM).^{33–37,20,38,39} ^bPotency range (0.13–460 nM).^{40,19,41,42} ^cPotency range (0.5 pM–1 μ M).^{43,27,44–74} ^dPotency range (25 nM–5 μ M).^{75–87}

decoys were prepared using LigPrep²³ in Maestro v9.5.²⁴ The Ionizer algorithm in LigPrep was used to generate tautomers at pH 7.4, and a maximum of eight stereoisomers were created when chiralities could not be determined. The decoy sets are all available in the Supporting Information.

The crystal structures with PDB IDs 1YT7 and 2F9U were used for Cathepsin K and HCV NS3 protease virtual screen, respectively. For EGFR we used representatives of active and inactive conformations (PDB IDs 2ITY and 1XKK). Two conformations of XPO1 were also selected, based on PDB ID

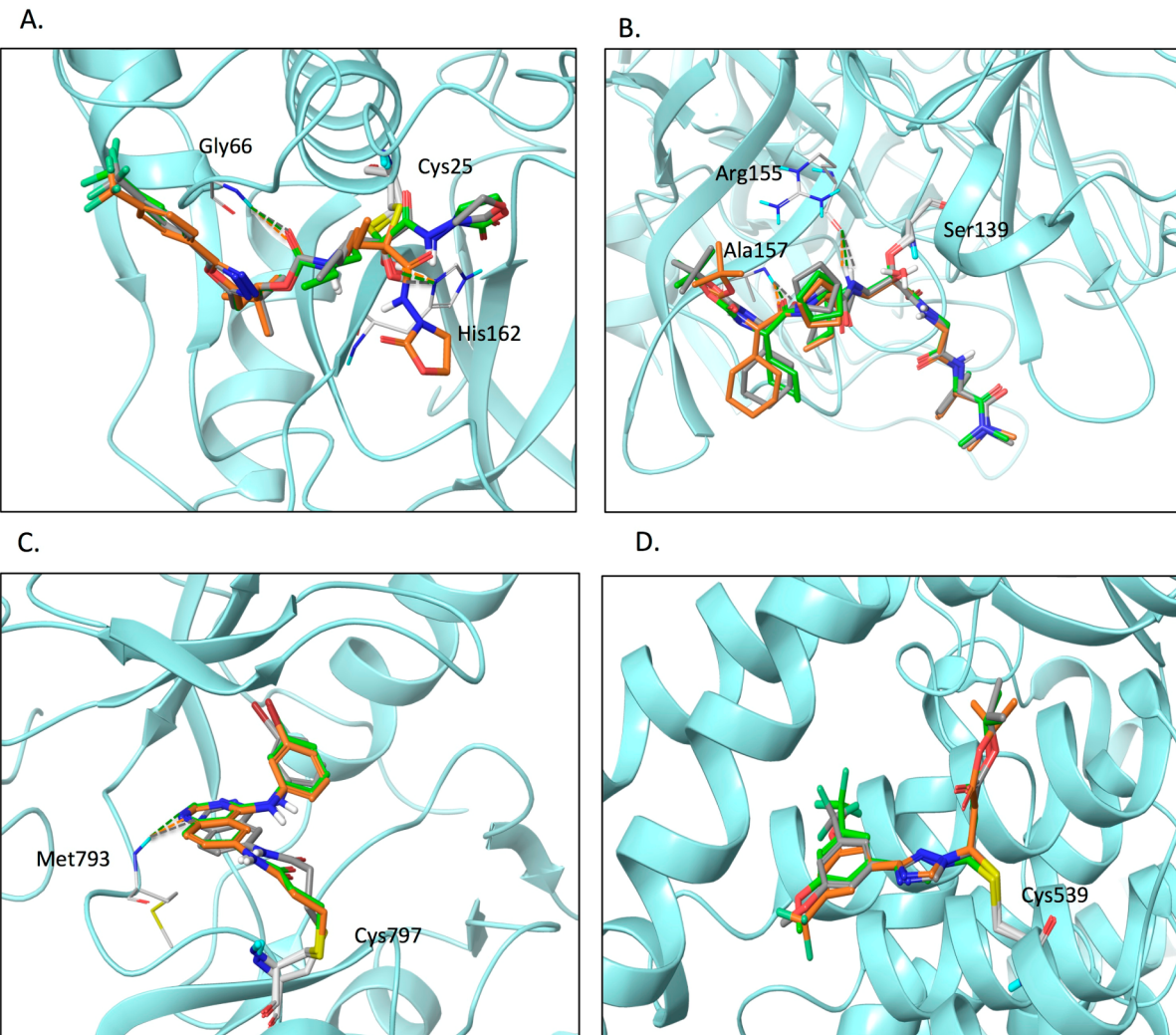


Figure 3. Comparison of selected poses using the CovDock-VS mode (orange) and CovDock-LO mode (green) to crystal structure (gray) for A) Cathepsin K structure (PDB ID 1YT7) with the cocrystal ligand, B) HCV NS3 protease structure (PDB ID 2F9U) with the cocrystal ligand, C) EGFR structure (PDB ID 2ITY) with the ligand 34-JAB, and D) XPO1 structure (PDB ID 4GMX) with the ligand K85 (KPT-185). The H-bond interactions used in postdocking filtering of the poses are shown in dashed lines (green: CovDock-LO mode pose, gray: crystal structure, orange: CovDock-VS mode pose). The residues interacting with the ligand and the attachment residues are shown in gray thin sticks.

4GMX and an additional, unpublished XPO1 structure (internal Karyopharm structure). Proteins were prepared using the Protein Preparation Wizard in Maestro v9.5.²⁵

RESULTS AND DISCUSSION

Retrospective SBVS using CovDock-VS described in the Methods section was performed on four targets: Cathepsin K, HCV NS3 protease, EGFR, and XPO1 (Table 1) which are representatives of 3 protein families, namely protease, kinase, and exportin families. In order to capture potential inhibitors that preferably bind to one protein conformation rather than another, ensemble docking has been used for EGFR and XPO1.²⁶ The two conformations selected for EGFR (PDB IDs 2ITY and 1XKK) represent the active and inactive states of the protein. The overall RMSD between these two conformations is 2.33 Å, with the major differences being the conformations of the Gly-loop and A-loop.²⁷ For XPO1 we used two closely related protein conformations that differ mainly in the rotamers of residues in the NES binding region. The same residues are also involved in the binding of XPO1 inhibitors as observed in XPO1 crystal structures containing KPT inhibitors.²⁸

For each docked compound, a maximum of 10 poses were saved and filtered based on hydrogen bonding (H-bond) interactions described in the literature for the known actives when relevant (Figure 3). For example, at least one H-bond between compounds docked to EGFR and residues in the hinge region (amino acids Q791-M793) was required based on the cocrystal structures of known irreversible EGFR inhibitors (such as PDB IDs 4I24, 4G5J, 3IKA and others). As described in the Methods section, the pose with the lowest GlideScore was saved and used for subsequent analysis.

This protocol resulted in viable poses satisfying the expected protein–ligand interactions for 81%, 72%, and 77% of the known actives of Cathepsin K, HCV NS3 protease, and EGFR, respectively. In the case of XPO1 no filter was applied as the interactions between the protein and known covalent inhibitors are mostly hydrophobic and weak nondirectional polar interactions. 95% of known XPO1 inhibitors were successfully docked using the CovDock-VS protocol, fitting the XPO1 binding site and fulfilling the hydrophobic interactions as observed in the crystal structures of XPO1 complexed with its known inhibitors (PDB IDs 4GMX, 4GPT, and others).

To evaluate the performance of the virtual screening procedure we used EF1%, EF10%, and BEDROC ($\alpha = 20$) metrics that are often used for evaluating virtual screening results²⁹ (Table 2). These metrics show that the CovDock-VS

Table 2. Evaluation of the VS Results

	EF1%	EF10%	BEDROC ($\alpha = 20$)
HCV NS3 protease	52	7	0.70
Cathepsin K	9	8	0.48
EGFR	46	8	0.65
XPO1	33	7	0.52

in conjunction with protein–ligand interaction filtering is a highly effective method in retrieving known covalently bound actives in the top percentile of a library of decoy compounds. The enrichment curves in Figure 4 graphically depict the

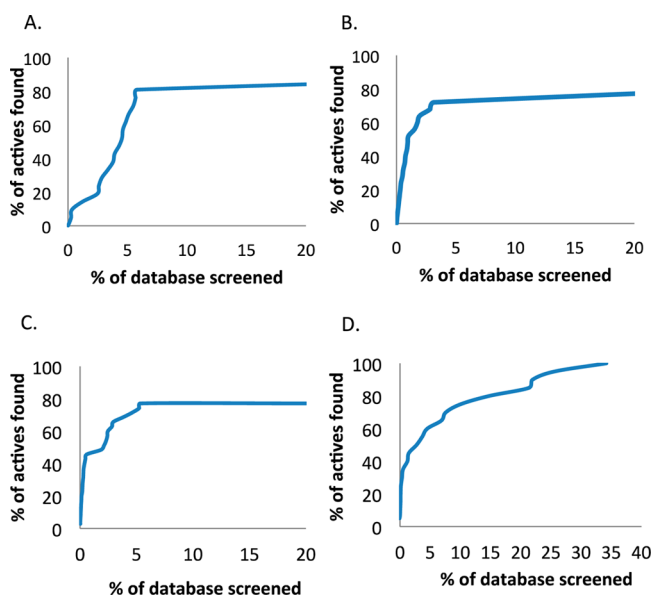


Figure 4. Enrichment curves: A) Cathepsin K, B) HCV NS3 protease, C) EGFR ensemble, and D) XPO1 ensemble.

quality of known active rankings compared to the decoys. All of the known actives that satisfied the H-bond filter were retrieved within the top 6% of the library screened for Cathepsin K, HCV NS3 protease, and EGFR. An interaction filter was not used in the case of XPO1, leading to a more gradual enrichment curve. Yet, nearly all actives (95%) are retrieved within 30% of a decoy library, and 33% of the known compounds are within 1% of a decoy library (EF1% = 33; Figure 4D).

The enrichment results worsen when H-bond filters are not used as postprocessing, with a 2.0-fold, 3.3-fold, and 1.2-fold decrease in EF1% and a 5.8-fold, 2.6-fold, and 1.3-fold decrease in EF10% for Cathepsin K, HCV NS3 protease, and EGFR, respectively. Improving the enrichment of actives using additional postprocessing filters demonstrates that our approach is able to sample the ligand and generate good poses. However, the scoring function we use (unmodified GlideScore) is not optimal for differentiating true actives from decoys with similar molecular properties as used in generating the decoy sets. This is possibly due to the fact that our approach does not account for differences in reactivity between candidate inhibitors as well as differences in the total energy of

the protein–ligand complex upon covalent bond formation. Such terms can possibly be approximated using quantum mechanical and free energy calculation methods, which would increase the computation time tremendously rendering the method unsuitable for SBVS. Therefore, CovDock-VS should be considered as a fast tool for generating VS quality binding modes combined with a reasonable ranking of noncovalent interactions that should be augmented by further filters to reduce false positive rates. Since this limitation is common to many SBVS campaigns,^{30–32} we do not see this as a setback.

Next we compared the quality of the binding modes generated by CovDock-VS and the slower and more accurate CovDock-LO for the known actives that have been cocrystallized. The docked poses were similar to the crystal structure with RMSDs less than 3.2 Å in both cases (Figure 3), but more poses had lower RMSDs in CovDock-LO mode (71% of the poses had RMSD < 2.0 Å in LO mode compared to 43% in VS mode). Furthermore, CovDock-LO was able to generate poses that satisfy the H-bond constraints for the boceprevir analogue S2 (PDB ID 3KNX), narpalaprevir (PDB ID 3LON), CVS4819 (PDB ID 2OC1), and neratinib (PDB ID 2JIV), while CovDock-VS failed in these cases (Figure 5, Table 3). In CovDock-LO, the selected poses are minimized using the Prime VSGB2.0 energy model,¹⁵ and Prime energy is used in ranking the poses. In CovDock-VS, this step is skipped, making the process approximately 10–40-fold faster depending on the protein and docked ligands, and the poses are ranked by their initial GlideScore. This difference accounts for the main differences in sampling and scoring between the two methods.

For most of the known EGFR and XPO1 inhibitors, the docking poses obtained using the CovDock-LO and VS modes were mostly similar, justifying evaluation of CovDock-VS as a tool for SBVS (Figure 3C and 3D).

In the absence of a tool for covalent SBVS, we have previously reported using an approach based on noncovalent docking of prereaction chemical structures using Glide combined with distance constraints between the reactive residue in the target protein and reactive atoms in the docked compounds.²⁶ We selected EGFR as a model system to compare CovDock-VS with the noncovalent Glide-based approach. The two docking procedures generated similar docked poses for 26 out of 35 known EGFR inhibitors. CovDock-VS binding modes were superior for seven of the nine remaining compounds (satisfying the H-bond filter), while noncovalent Glide produced better binding modes only for two. Furthermore, CovDock-VS resulted in significantly better enrichment results (Figure 6).

CONCLUSION

Structure-based virtual screening (SBVS) is valuable for identifying novel small molecules that bind to protein targets. However, while this technology is widely applied for the identification of noncovalent binders, SBVS for covalent inhibitors discovery has been mostly hampered by scalability and docking speed limitations. The new covalent docking workflow developed by Schrödinger (CovDock) combines Glide docking and Prime optimization to generate covalent protein–ligand complexes. It requires minimal user effort in preparing the necessary input files since many common covalent attachment reactions (e.g., Michael addition, Nucleophilic addition, Beta Lactam addition, etc.) are predefined. Also, the reactive atoms are automatically recognized by specifying the reaction and SMARTS pattern defining the

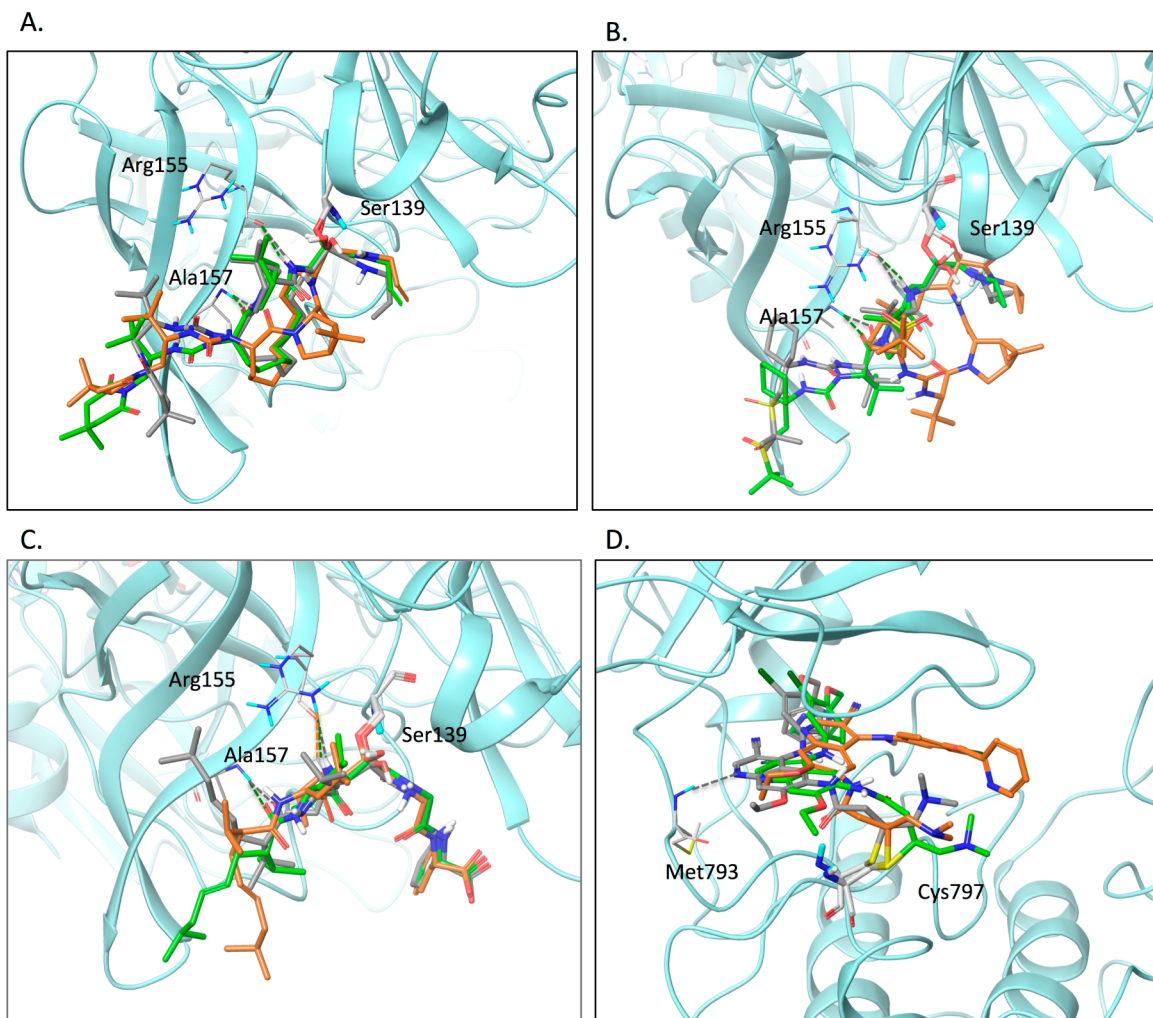


Figure 5. Comparison of docked poses of compounds for which none of the poses satisfied the postdocking H-bond filters. CovDock-VS mode (orange), CovDock-LO mode (green), crystal structure (gray). A) HCV NS3 protease 3KNX ligand (boceprevir analogue 52), B) HCV NS3 protease 3LON ligand (narlaprevir), C) HCV NS3 protease 2OC1 ligand (CVS4819), and D) EGFR 2JIV ligand (Neratinib). The H-bond interactions used in postdocking filtering of the poses are shown in dashed lines (green: CovDock-LO mode pose, gray: crystal structure, orange: CovDock-VS mode pose). The H-bonding residues and the attachment residues are shown in gray thin sticks. Protein carbons of the crystal structure are colored gray. The absence of orange or green dashed lines depicts that the CovDock-VS mode or CovDock-LO mode poses did not pass the H-bond filter.

warheads.¹⁴ This approach has been shown to be useful for pose prediction and also for differentiating actives from inactive ligands, which is crucial in Virtual Screening and Lead Optimization. However, the calculation of the affinity score,¹⁴ which is the default scoring function in the Schrödinger CovDock program, is not fast enough for screening large numbers of molecules especially when the computational resources are limited.

In this work, we present a modified algorithm derived from the CovDock-LO mode, designed to enable screening of large compound collections containing a variety of chemical warheads. The settings we have chosen, which we refer to as the CovDock-VS mode, significantly improves the speed (10–40-fold) causing minor deterioration in the accuracy of the predicted poses when compared to available protein–ligand cocrystal structures (mean RMSD 1.9 Å in CovDock-VS mode compared to 1.5 Å in CovDock-LO mode). Zhu et al.¹⁴ showed that using affinity score would be favorable for pose prediction and enrichment studies compared to just initial GlideScore; however, this approach would have increased the computation

time making the screening of large libraries less realistic. Here, we show that by using the Covalent Docking in VS mode in conjunction with interaction filters (in this case, H-bond constraints), we were able to retrieve 71%, 72%, and 77% of the known actives for Cathepsin K, HCV NS3 protease, and EGFR within 5% of the decoy library, respectively. Even when interaction filters could not be used, as for XPO1, we were still able to retrieve 95% of the actives within 30% of the decoy library for XPO1, with 33% and 57% of the known compounds included in 1% and 5% of the decoys, respectively.

In conclusion, the default CovDock workflow has been successfully modified to suit the requirements of covalent SBVS by improving the speed of the calculations significantly without extensively compromising the accuracy of the predicted ligand poses as well as compound ranking. We therefore propose CovDock-VS as a widely applicable tool for identification of novel and diverse covalent binders in SBVS projects.

Table 3. RMSDs of Ligand Heavy Atoms the Known Active Poses Generated Using the CovDock VS and LO Modes Compared to the Crystal Structure

	CovDock-VS	CovDock-LO
Cathepsin K Actives		
1YT7-ligand ^c	2.68	0.68
2BDL-ligand	2.48	2.89 ^a
1TU6-ligand	1.43	3.18
HCV NS3 Protease Actives		
3KNX-ligand	2.89 ^a	2.45
2GVF-ligand	1.66	1.51
3LON-ligand	6.69 ^a	1.81
2OC7-ligand	1.38	1.12
2F9U-ligand ^c	1.19	1.30
2OBO-ligand	1.29	0.98
2OC8-ligand	1.55	1.04
2A4Q-ligand	2.51	2.28
2OC0-ligand	3.03	0.88
3LOX-ligand	2.07	1.72
2OC1-ligand	3.75 ^a	3.14
EGFR Actives		
4I24-ligand (Dacomitinib)	1.46	0.85
4GSJ-ligand (Afatinib)	1.81	0.86
3IKA-ligand (WZ4002)	2.53 ^a	1.67
2JIV-ligand (Neratinib)	6.54 ^a	2.41 ^a
2JSF-ligand (34-JAB)	1.57	1.20
XPO1 Actives		
4GMX-ligand (KPT-185) ^c	2.19 ^b	0.67
KPT-276 (not submitted to PDB) ^c	2.54 ^a	1.07
mean	1.87	1.50

^aRMSDs for poses with lowest GlideScore are reported for the ligands that did not satisfy the postdocking H-bond filters. These are excluded from the mean RMSD calculations. ^bFlip of $-OMe$ and $-CF_3$ groups.

^cSelf-docking of the cocrystal ligands to the protein structures used in VS.

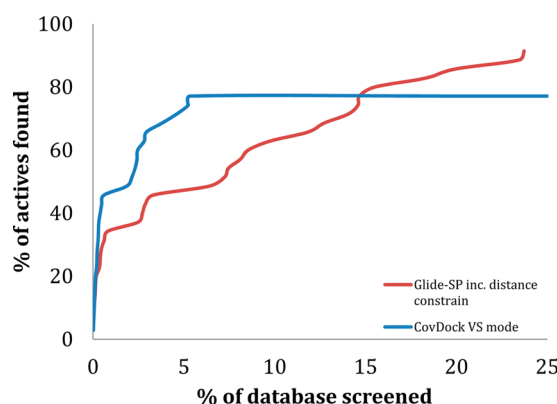


Figure 6. Enrichment results for Glide (including distance constraint as described in the text) in comparison with the new CovDock-VS mode, colored red and blue, respectively. In both cases postdocking H-bond filter was applied.

ASSOCIATED CONTENT

Supporting Information

Physicochemical properties of the decoys and actives used in virtual screening (Figure S1); chemical structures of the known active molecules used in the enrichment studies (Figure S2); decoy sets used in virtual screening. This material is available free of charge via the Internet at <http://pubs.acs.org>.

AUTHOR INFORMATION

Corresponding Author

*E-mail: ori@karyopharm.com.

Author Contributions

[§]D.T.W and G.G.: These authors contributed equally to this work.

Notes

The authors declare no competing financial interest.

ACKNOWLEDGMENTS

We thank Woody Sherman for helpful discussions and critical comments on the manuscript. We also would like to acknowledge the contribution of Erkan Baloglu and Vincent Sandanayaka to the synthesis of KPT compounds shown in Figure S1.D.

REFERENCES

- (1) Robertson, J. G. Mechanistic Basis of Enzyme-Targeted Drugs. *Biochemistry* **2005**, *44*, 5561–5571.
- (2) Stachulski, A. V.; Baillie, T. A.; Park, B. K.; Obach, R. S.; Dalvie, D. K.; Williams, D. P.; Srivastava, A.; Regan, S. L.; Antoine, D. J.; Goldring, C. E. P.; Chia, A. J. L.; Kitteringham, N. R.; Randle, L. E.; Callan, H.; Castrejon, J. L.; Farrell, J.; Naisbitt, D. J.; Lennard, M. S. The Generation, Detection, and Effects of Reactive Drug Metabolites. *Med. Res. Rev.* **2013**, *33*, 985–1080.
- (3) Lapalombella, R.; Sun, Q.; Williams, K.; Tangeman, L.; Jha, S.; Zhong, Y.; Goettl, V.; Mahoney, E.; Berglund, C.; Gupta, S.; Farmer, A.; Mani, R.; Johnson, A. J.; Lucas, D.; Mo, X.; Daelemans, D.; Sandanayaka, V.; Shechter, S.; McCauley, D.; Shacham, S.; Kauffman, M.; Chook, Y. M.; Byrd, J. C. Selective Inhibitors of Nuclear Export Show That CRM1/XPO1 Is a Target in Chronic Lymphocytic Leukemia. *Blood* **2012**, *120*, 4621–4634.
- (4) Serafimova, I. M.; Pufall, M. A.; Krishnan, S.; Duda, K.; Cohen, M. S.; Maglathlin, R. L.; et al. Reversible targeting of noncatalytic cysteines with chemically tuned electrophiles. *Nat. Chem. Biol.* **2012**, *8* (5), 471–476.
- (5) Friesner, R. A.; Banks, J. L.; Murphy, R. B.; Halgren, T. A.; Klicic, J. J.; Mainz, D. T.; Repasky, M. P.; Knoll, E. H.; Shelley, M.; Perry, J. K.; Shaw, D. E.; Francis, P.; Shenkin, P. S. Glide: a New Approach for Rapid, Accurate Docking and Scoring. 1. Method and Assessment of Docking Accuracy. *J. Med. Chem.* **2004**, *47*, 1739–1749.
- (6) Halgren, T. A.; Murphy, R. B.; Friesner, R. A.; Beard, H. S.; Frye, L. L.; Pollard, W. T.; Banks, J. L. Glide: a New Approach for Rapid, Accurate Docking and Scoring. 2. Enrichment Factors in Database Screening. *J. Med. Chem.* **2004**, *47*, 1750–1759.
- (7) Jones, G.; Willett, P.; Glen, R. C.; Leach, A. R.; Taylor, R. Development and validation of a genetic algorithm for flexible docking. *J. Mol. Biol.* **1997**, *267*, 727–748.
- (8) Jones, G.; Willett, P.; Glen, R. C. Molecular Recognition of Receptor Sites Using a Genetic Algorithm with a Description of Desolvation. *J. Mol. Biol.* **1995**, *245*, 43–53.
- (9) Morris, G. M.; Huey, R.; Lindstrom, W.; Sanner, M. F.; Belew, R. K.; Goodsell, D. S.; Olson, A. J. AutoDock4 and AutoDockTools4: Automated Docking with Selective Receptor Flexibility. *J. Comput. Chem.* **2009**, *30*, 2785–2791.
- (10) Rarey, M.; Kramer, B.; Lengauer, T.; Klebe, G. A Fast Flexible Docking Method Using an Incremental Construction Algorithm. *J. Mol. Biol.* **1996**, *261*, 470–489.
- (11) McInnes, C. Improved Lead-Finding for Kinase Targets Using High-Throughput Docking. *Curr. Opin. Drug Discovery Dev.* **2006**, *9*, 339–347.
- (12) Ouyang, X.; Zhou, S.; Su, C. T. T.; Ge, Z.; Li, R.; Kwoh, C. K. CovalentDock: Automated Covalent Docking with Parameterized Covalent Linkage Energy Estimation and Molecular Geometry Constraints. *J. Comput. Chem.* **2013**, *34*, 326–336.

- (13) Schröder, J.; Klinger, A.; Oellien, F.; Marhöfer, R. J.; Duszenko, M.; Selzer, P. M. Docking-Based Virtual Screening of Covalently Binding Ligands: an Orthogonal Lead Discovery Approach. *J. Med. Chem.* **2013**, *56*, 1478–1490.
- (14) Zhu, K.; Borrelli, W. K.; Greenwood, J. R.; Day, T.; Abel, R.; Farid, R. S.; Harder, E. Docking Covalent Inhibitors: a Parameter Free Approach to Pose Prediction and Scoring. *J. Chem. Inf. Model.* **2014**, DOI: 10.1021/ci500118s.
- (15) Li, J.; Abel, R.; Zhu, K.; Cao, Y.; Zhao, S.; Friesner, R. A. The VSGB 2.0 Model: a Next Generation Energy Model for High Resolution Protein Structure Modeling. *Proteins* **2011**, *79*, 2794–2812.
- (16) Watts, K. S.; Dalal, P.; Murphy, R. B.; Sherman, W.; Friesner, R. A.; Shelley, J. C. ConfGen: a Conformational Search Method for Efficient Generation of Bioactive Conformers. *J. Chem. Inf. Model.* **2010**, *50*, 534–546.
- (17) Jorgensen, W. L.; Maxwell, D. S.; Tirado-Rives, J. Development and Testing of the OPLS All-Atom Force Field on Conformational Energetics and Properties of Organic Liquids. *J. Am. Chem. Soc.* **1996**, *118*, 11225–11236.
- (18) Shrivakumar, D.; Williams, J.; Wu, Y.; Damm, W.; Shelley, J.; Sherman, W. Prediction of Absolute Solvation Free Energies Using Molecular Dynamics Free Energy Perturbation and the OPLS Force Field. *J. Chem. Theory Comput.* **2010**, *6*, 1509–1519.
- (19) Barrett, D. G.; Boncek, V. M.; Catalano, J. G.; Deaton, D. N.; Hassell, A. M.; Jurgensen, C. H.; Long, S. T.; McFadyen, R. B.; Miller, A. B.; Miller, L. R.; Payne, J. A.; Ray, J. A.; Samano, V.; Shewchuk, L. M.; Tavares, F. X.; Wells-Knecht, K. J.; Willard, D. H., Jr.; Wright, L. L.; Zhou, H.-Q. Q. P2–P3 Conformationally Constrained Ketoamide-Based Inhibitors of Cathepsin K. *Bioorg. Med. Chem. Lett.* **2005**, *15*, 3540–3546.
- (20) Arasappan, A.; Njoroge, F. G.; Chen, K. X.; Venkatraman, S.; Parekh, T. N.; Gu, H.; Pichardo, J.; Butkiewicz, N.; Prongay, A.; Madison, V.; Girijavallabhan, V. P2–P4 Macroyclic inhibitors of hepatitis C virus NS3–4A serine protease. *Bioorg. Med. Chem. Lett.* **2006**, *16*, 3960–3965.
- (21) Carmi, C.; Mor, M.; Petronini, P. G.; Alfieri, R. R. Clinical Perspectives for Irreversible Tyrosine Kinase Inhibitors in Cancer. *Biochem. Pharmacol.* **2012**, *84*, 1388–1399.
- (22) Pierce, A. C.; Rao, G.; Bemis, G. W. BREED: Generating Novel Inhibitors Through Hybridization of Known Ligands. Application to CDK2, P38, and HIV Protease. *J. Med. Chem.* **2004**, *47*, 2768–2775.
- (23) LigPrep v2.7. Schrodinger, Inc.: Portland, 2013.
- (24) Maestro v9.5. Schrodinger, Inc.: Portland, 2013.
- (25) Sastry, G. M.; Adzhigirey, M.; Day, T.; Annabhimoju, R.; Sherman, W. Protein and Ligand Preparation: Parameters, Protocols, and Influence on Virtual Screening Enrichments. *J. Comput.-Aided Mol. Des.* **2013**, *27*, 221–234.
- (26) Kalid, O.; Toledo Warshaviak, D.; Shechter, S.; Sherman, W.; Shacham, S. Consensus Induced Fit Docking (cIFD): methodology, validation, and application to the discovery of novel Crm1 inhibitors. *J. Comput.-Aided Mol. Des.* **2012**, *26*, 1217–1228.
- (27) Zhou, W.; Ercan, D.; Chen, L.; Yun, C.-H.; Li, D.; Capelletti, M.; Cortot, A. B.; Chiriac, L.; Iacob, R. E.; Padera, R.; Engen, J. R.; Wong, K.-K.; Eck, M. J.; Gray, N. S.; Jänne, P. A. Novel Mutant-Selective EGFR Kinase Inhibitors Against EGFR T790M. *Nature* **2009**, *462*, 1070–1074.
- (28) Etchin, J.; Sun, Q.; Kentsis, A.; Farmer, A.; Zhang, Z. C.; Sanda, T.; Mansour, M. R.; Barcelo, C.; McCauley, D.; Kauffman, M.; Shacham, S.; Christie, A. L.; Kung, A. L.; Rodig, S. J.; Chook, Y. M.; Look, A. T. Antileukemic Activity of Nuclear Export Inhibitors That Spare Normal Hematopoietic Cells. *Leukemia* **2013**, *27*, 66–74.
- (29) Truchon, J.-F.; Bayly, C. I. Evaluating Virtual Screening Methods: Good and Bad Metrics for the “Early Recognition” Problem. *J. Chem. Inf. Model.* **2007**, *47*, 488–508.
- (30) Kroemer, R. T. Structure-Based Drug Design: Docking and Scoring. *Curr. Protein Pept. Sci.* **2007**, *8*, 312–328.
- (31) Li, Y. Y.; An, J.; Jones, S. J. M. A Computational Approach to Finding Novel Targets for Existing Drugs. *PLoS Comput. Biol.* **2011**, *7*, e1002139.
- (32) Sela, I.; Golan, G.; Strajbl, M.; Rivenzon-Segal, D.; Bar-Haim, S.; Bloch, I.; Inbal, B.; Shitrit, A.; Ben-Zeev, E.; Fichman, M.; Markus, Y.; Marantz, Y.; Senderowitz, H.; Kalid, O. G Protein Coupled Receptors - in Silico Drug Discovery and Design. *Curr. Top. Med. Chem. (Sharjah, United Arab Emirates)* **2010**, *10*, 638–656.
- (33) Bennett, F.; Huang, Y.; Hendrata, S.; Lovey, R.; Bogen, S. L.; Pan, W.; Guo, Z.; Prongay, A.; Chen, K. X.; Arasappan, A.; Venkatraman, S.; Velazquez, F.; Nair, L.; Sannigrahi, M.; Tong, X.; Pichardo, J.; Cheng, K.-C.; Girijavallabhan, V. M.; Saksena, A. K.; Njoroge, F. G. The Introduction of P4 Substituted 1-Methylcyclohexyl Groups Into Boceprevir: a Change in Direction in the Search for a Second Generation HCV NS3 Protease Inhibitor. *Bioorg. Med. Chem. Lett.* **2010**, *20*, 2617–2621.
- (34) Prongay, A. J.; Guo, Z.; Yao, N.; Pichardo, J.; Fischmann, T.; Strickland, C.; Myers, J.; Weber, P. C.; Beyer, B. M.; Ingram, R.; Hong, Z.; Prosise, W. W.; Ramanathan, L.; Taremi, S. S.; Yarosh-Tomaine, T.; Zhang, R.; Senior, M.; Yang, R.-S.; Malcolm, B.; Arasappan, A.; Bennett, F.; Bogen, S. L.; Chen, K.; Jao, E.; Liu, Y.-T.; Lovey, R. G.; Saksena, A. K.; Venkatraman, S.; Girijavallabhan, V.; Njoroge, F. G.; Madison, V. Discovery of the HCV NS3/4A Protease Inhibitor (1R,SS)-N-[3-Amino-1-(Cyclobutylmethyl)-2,3-Dioxopropyl]-3-[2(S)-[[[(1,1-Dimethylethyl)Amino]Carbonyl]Amino]-3,3-Dimethyl-1-Oxobutyl]-6,6-Dimethyl-3-Azabicyclo[3.1.0]Hexan-2(S)-Carboxamide (Sch 503034) II. Key Steps in Structure-Based Optimization. *J. Med. Chem.* **2007**, *50*, 2310–2318.
- (35) Chen, K. X.; Njoroge, F. G.; Prongay, A.; Pichardo, J. Synthesis and Biological Activity of Macroyclic Inhibitors of Hepatitis C Virus (HCV) NS3 Protease. *Bioorg. Med. Chem. Lett.* **2005**, *15*, 4475–4478.
- (36) Venkatraman, S.; Bogen, S. L.; Arasappan, A.; Bennett, F.; Chen, K.; Jao, E.; et al. Discovery of (1R,SS)-N-[3-Amino-1-(cyclobutylmethyl)-2,3-dioxopropyl]-3-[2(S)-[[[(1,1-dimethylethyl)amino]carbonyl]amino]-3,3-dimethyl-1-oxobutyl]-6,6-dimethyl-3-azabicyclo[3.1.0]hexan-2(S)-carboxamide (SCH 503034), a Selective, Potent, Orally Bioavailable Hepatitis C Virus NS3 Protease Inhibitor: A Potential Therapeutic Agent for the Treatment of Hepatitis C Infection. *J. Med. Chem.* **2006**, *49*, 6074–6086.
- (37) Arasappan, A.; Bennett, F.; Bogen, S. L.; Venkatraman, S.; Blackman, M.; Chen, K. X.; et al. Discovery of Narlaprevir (SCH 900518): A Potent, Second Generation HCV NS3 Serine Protease Inhibitor. *ACS Med. Chem. Lett.* **2010**, *1*, 64–69.
- (38) Venkatraman, S.; Velazquez, F.; Wu, W.; Blackman, M.; Chen, K. X.; Bogen, S.; Nair, L.; Tong, X.; Chase, R.; Hart, A.; Agrawal, S.; Pichardo, J.; Prongay, A.; Cheng, K.-C.; Girijavallabhan, V.; Piwinski, J.; Shih, N.-Y.; Njoroge, F. G. Discovery and Structure–Activity Relationship of P1–P3 Ketoamide Derived Macroyclic Inhibitors of Hepatitis C Virus NS3 Protease. *J. Med. Chem.* **2009**, *52*, 336–346.
- (39) Venkatraman, S.; Njoroge, F. G.; Wu, W.; Girijavallabhan, V.; Prongay, A. J.; Butkiewicz, N.; Pichardo, J. Novel inhibitors of hepatitis C NS3–NS4A serine protease derived from 2-aza-bicyclo[2.2.1]-heptane-3-carboxylic acid. *Bioorg. Med. Chem. Lett.* **2006**, *16*, 1628–1632.
- (40) Barrett, D. G.; Catalano, J. G.; Deaton, D. N.; Long, S. T.; Miller, L. R.; Tavares, F. X.; et al. Orally bioavailable small molecule ketoamide-based inhibitors of cathepsin K. *Bioorg. Med. Chem. Lett.* **2004**, *14*, 4897–4902.
- (41) Barrett, D. G.; Catalano, J. G.; Deaton, D. N.; Hassell, A. M.; Long, S. T.; Miller, A. B.; Miller, L. R.; Ray, J. A.; Samano, V.; Shewchuk, L. M.; Wells-Knecht, K. J.; Willard, D. H.; Wright, L. L. Novel, Potent P2-P3 Pyrrolidine Derivatives of Ketoamide-Based Cathepsin K Inhibitors. *Bioorg. Med. Chem. Lett.* **2006**, *16*, 1735–1739.
- (42) Tavares, F. X.; Boncek, V.; Deaton, D. N.; Hassell, A. M.; Long, S. T.; Miller, A. B.; et al. Design of Potent, Selective, and Orally Bioavailable Inhibitors of Cysteine Protease Cathepsin K. *J. Med. Chem.* **2004**, *47*, 588–599.
- (43) Gajiwala, K. S.; Feng, J.; Ferre, R.; Ryan, K.; Brodsky, O.; Weinrich, S.; Kath, J. C.; Stewart, A. Insights Into the Aberrant Activity of Mutant EGFR Kinase Domain and Drug Recognition. *Structure* **2013**, *21*, 209–219.

- (44) Solca, F.; Dahl, G.; Zoephel, A.; Bader, G.; Sanderson, M.; Klein, C.; Kraemer, O.; Himmelsbach, F.; Haaksma, E.; Adolf, G. R. Target Binding Properties and Cellular Activity of Afatinib (BIBW 2992), an Irreversible ErbB Family Blocker. *J. Pharmacol. Exp. Ther.* **2012**, *343*, 342–350.
- (45) Ako, E.; Yamashita, Y.; Ohira, M.; Yamazaki, M.; Hori, T.; Kubo, N.; Sawada, T.; Hirakawa, K. The Pan-erbB Tyrosine Kinase Inhibitor CI-1033 Inhibits Human Esophageal Cancer Cells in Vitro and in Vivo. *Oncol. Rep.* **2000**, *17*, 887–893.
- (46) Rabindran, S. K. Antitumor Activity of HKI-272, an Orally Active, Irreversible Inhibitor of the HER-2 Tyrosine Kinase. *Cancer Res.* **2004**, *64*, 3958–3965.
- (47) Discafani, C. M.; Carroll, M. L.; Floyd, M. B., Jr.; Hollander, I. J.; Husain, Z.; Johnson, B. D.; Kitchen, D.; May, M. K.; Malo, M. S.; Minnick, A. A., Jr.; Nilakantan, R.; Shen, R.; Wang, Y.-F.; Wissner, A.; Greenberger, L. M. Irreversible Inhibition of Epidermal Growth Factor Receptor Tyrosine Kinase with in Vivo Activity by N-[4-[(3-Bromophenyl)Amino]-6-Quinazolinyl]-2-Butynamide (CL-387,785). *Biochem. Pharmacol.* **1999**, *57*, 917–925.
- (48) Blair, J. A.; Rauh, D.; Kung, C.; Yun, C.-H.; Fan, Q.-W.; Rode, H.; Zhang, C.; Eck, M. J.; Weiss, W. A.; Shokat, K. M. Structure-Guided Development of Affinity Probes for Tyrosine Kinases Using Chemical Genetics. *Nat. Chem. Biol.* **2007**, *3*, 229–238.
- (49) Sun, Y.; Fry, D. W.; Vincent, P.; Nelson, J. M.; Elliot, W.; Leopold, W. R. Growth inhibition of nasopharyngeal carcinoma cells by EGF receptor tyrosine kinase inhibitors. *Anticancer Res.* **1999**, *19*, 919–924.
- (50) Barf, T.; Kaptein, A. Irreversible Protein Kinase Inhibitors: Balancing the Benefits and Risks. *J. Med. Chem.* **2012**, *55*, 6243–6262.
- (51) Boschelli, D. 4-Anilino-3-Quinolinecarbonitriles: an Emerging Class of Kinase Inhibitors. *Curr. Top. Med. Chem. (Sharjah, United Arab Emirates)* **2002**, *2*, 1051–1063.
- (52) Ghosh, S.; Zheng, Y.; Jun, X.; Mahajan, S.; Mao, C.; Sudbeck, E. A.; Uckun, F. M. Specificity of α -Cyano- β -Hydroxy- β -Methyl-N-[4-(Trifluoromethoxy)Phenyl]-Propenamide as an Inhibitor of the Epidermal Growth Factor Receptor Tyrosine Kinase. *Clin. Cancer Res.* **1999**, *5*, 4264–4272.
- (53) Dowlati, A.; Nethery, D.; Kern, J. A. Combined inhibition of epidermal growth factor receptor and JAK/STAT pathways results in greater growth inhibition in vitro than single agent therapy. *Mol. Cancer Ther.* **2004**, *3* (4), 459–463.
- (54) Xie, H.; Lin, L.; Tong, L.; Jiang, Y.; Zheng, M.; Chen, Z.; Jiang, X.; Zhang, X.; Ren, X.; Qu, W.; Yang, Y.; Wan, H.; Chen, Y.; Zuo, J.; Jiang, H.; Geng, M.; Ding, J. AST1306, a Novel Irreversible Inhibitor of the Epidermal Growth Factor Receptor 1 and 2, Exhibits Antitumor Activity Both in Vitro and in Vivo. *PLoS One* **2011**, *6*, e21487.
- (55) Honigberg, L.; Verner, E. J.; Buggy, J. J.; Loury, D. J.; Chen, W. Inhibitors of Bruton's Tyrosine Kinase, US Patent 20130035334 A1, Feb 7, 2013.
- (56) Kim, K.-H.; Maderna, A.; Schnute, M. E.; Hegen, M.; Mohan, S.; Miyashiro, J.; Lin, L.; Li, E.; Keegan, S.; Lussier, J.; Wrocklage, C.; Nickerson-Nutter, C. L.; Wittwer, A. J.; Souter, H.; Caspers, N.; Han, S.; Kurumbail, R.; Dunussi-Joannopoulos, K.; Douhan, J., III; Wissner, A. Imidazo[1,5-a]Quinoxalines as Irreversible BTK Inhibitors for the Treatment of Rheumatoid Arthritis. *Bioorg. Med. Chem. Lett.* **2011**, *21*, 6258–6263.
- (57) Singh, J.; Ghosh, S.; Kluge, A. F.; Petter, R. C.; Tester, R. W. 4,6-Disubstituted Pyrimidines Useful as Kinase Inhibitors, US Patent 7989465 B2, Aug 2, 2011.
- (58) Chen, W.; Loury, D. J. Pyrazolo[3,4-D]Pyrimidine and Pyrrolo[2,3-D]Pyrimidine Compounds as Kinase Inhibitors, US Patent 8377946 B1, Feb 19, 2013.
- (59) Honigberg, L.; Verner, E. J.; Buggy, J. J.; Loury, D. J.; Chen, W. Inhibitors of BMX Non-Receptor Tyrosine Kinase, US Patent 20120184013 A1, Jul 19, 2012.
- (60) Honigberg, L. A.; Smith, A. M.; Sirisawad, M.; Verner, E.; Loury, D.; Chang, B.; Li, S.; Pan, Z.; Thamm, D. H.; Miller, R. A.; Buggy, J. J. The Bruton Tyrosine Kinase Inhibitor PCI-32765 Blocks B-Cell Activation and Is Efficacious in Models of Autoimmune Disease and B-Cell Malignancy. *Proc. Natl. Acad. Sci. U. S. A.* **2010**, *107*, 13075–13080.
- (61) Cha, M. Y.; Lee, K.-O.; Kim, M.; Song, J. Y.; Lee, K. H.; Park, J.; Chae, Y. J.; Kim, Y. H.; Suh, K. H.; Lee, G. S.; Park, S. B.; Kim, M. S. Antitumor Activity of HM781-36B, a Highly Effective Pan-HER Inhibitor in Erlotinib-Resistant NSCLC and Other EGFR-Dependent Cancer Models. *Int. J. Cancer* **2011**, *130*, 2445–2454.
- (62) Singh, J.; Petter, R. C.; Tester, R. W.; Kluge, A. F.; Mazdiyasni, H.; Westin, W. F.; Niu, D.; Qiao, L. Heteroaryl Compounds and Uses Thereof, US Patent 20130065879 A1, Mar 14, 2013.
- (63) Lee, K.; Niu, D.; Baevsky, M. F. Mutant-Selective Egfr Inhibitors and Uses Thereof, US Patent 20120157426 A1, Jun 21, 2012.
- (64) Wang, H. Q. Epidermal Growth Factor Receptor-Dependent, NF- B-Independent Activation of the Phosphatidylinositol 3-Kinase/Akt Pathway Inhibits Ultraviolet Irradiation-Induced Caspases-3, -8, and -9 in Human Keratinocytes. *J. Biol. Chem.* **2003**, *278*, 45737–45745.
- (65) Wissner, A.; Hamann, P. R.; Nilakantan, R.; Greenberger, L. M.; Ye, F.; Rapuano, T. A.; Loganzo, F. Syntheses and EGFR Kinase Inhibitory Activity of 6-Substituted-4-Anilino [1,7] and [1,8] Naphthyridine-3-Carbonitriles. *Bioorg. Med. Chem. Lett.* **2004**, *14*, 1411–1416.
- (66) Wu, C.-H.; Coumar, M. S.; Chu, C.-Y.; Lin, W.-H.; Chen, Y.-R.; Chen, C.-T.; et al. Design and Synthesis of Tetrahydropyridothieno-[2,3-d]pyrimidine Scaffold Based Epidermal Growth Factor Receptor (EGFR) Kinase Inhibitors: The Role of Side Chain Chirality and Michael Acceptor Group for Maximal Potency. *J. Med. Chem.* **2010**, *53*, 7316–7326.
- (67) Coumar, M. S.; Chu, C.-Y.; Lin, C.-W.; Shiao, H.-Y.; Ho, Y.-L.; Reddy, R.; Lin, W.-H.; Chen, C.-H.; Peng, Y.-H.; Leou, J.-S.; Lien, T.-W.; Huang, C.-T.; Fang, M.-Y.; Wu, S.-H.; Wu, J.-S.; Chittimalla, S. K.; Song, J.-S.; Hsu, J. T. A.; Wu, S.-Y.; Liao, C.-C.; Chao, Y.-S.; Hsieh, H.-P. Fast-Forwarding Hit to Lead: Aurora and Epidermal Growth Factor Receptor Kinase Inhibitor Lead Identification. *J. Med. Chem.* **2010**, *53*, 4980–4988.
- (68) Chang, S.; Zhang, L.; Xu, S.; Luo, J.; Lu, X.; Zhang, Z.; Xu, T.; Liu, Y.; Tu, Z.; Xu, Y.; Ren, X.; Geng, M.; Ding, J.; Pei, D.; Ding, K. Design, Synthesis, and Biological Evaluation of Novel Conformationally Constrained Inhibitors Targeting Epidermal Growth Factor Receptor Threonine 790→ Methionine 790 Mutant. *J. Med. Chem.* **2012**, *55*, 2711–2723.
- (69) Suzuki, T.; Fujii, A.; Ohya, J.; Amano, Y.; Kitano, Y.; Abe, D.; Nakamura, H. Pharmacological Characterization of MP-412 (AV-412), a Dual Epidermal Growth Factor Receptor and ErbB2 Tyrosine Kinase Inhibitor. *Cancer Sci.* **2007**, *98*, 1977–1984.
- (70) Butterworth, S.; Finlay, M. R. V.; Ward, R. A.; Kadambur, V. K.; Murugan, C. R. C.; Murugan, A.; Redfearn, H. M. 2-(2,4,5-Substituted-Anilino) Pyrimidine Compounds, US Patent 20130053409 A1, Feb 28, 2013.
- (71) Fakhouri, S.; Lee, H.; Reed, J.; Schlosser, K.; Sexton, K.; Tecle, H.; Winters, R. 4-Phenylamino-Quinazolin-6-Yl-Amides, US Patent 20050250761 A1, Nov 10, 2005.
- (72) Cheng, H.; Johnson, T. O.; Kath, J. C.; Liu, K. K. C.; Lunney, E. A.; Nagata, A.; Nair, S. K.; Planken, S. P.; Sutton, S. C. Pyrrolopyrimidine and Purine Derivatives, US Patent 20130079324 A1, Mar 28, 2013.
- (73) Fry, D. W.; Bridges, A. J.; Denny, W. A.; Doherty, A.; Greis, K. D.; Hicks, J. L.; Hook, K. E.; Keller, P. R.; Leopold, W. R.; Loo, J. A.; McNamara, D. J.; Nelson, J. M.; Sherwood, V.; Smail, J. B.; Trumpp-Kallmeyer, S.; Dobrusin, E. M. Specific, Irreversible Inactivation of the Epidermal Growth Factor Receptor and erbB2, by a New Class of Tyrosine Kinase Inhibitor. *Proc. Natl. Acad. Sci. U. S. A.* **1998**, *95*, 12022–12027.
- (74) Cha, M. Y.; Jung, Y. H.; Kang, S. J.; Kim, E. Y.; Kim, M. S.; Kim, M. R.; Kim, S. Y.; Kim, Y. H.; Lee, K. O.; Song, J. Y. Novel Pyrimidine Derivative for Inhibiting the Growth of Cancer Cells, WO Patent 2011099764 A3, Jan 5, 2012.
- (75) Internal data from Karyopharm Therapeutics.

- (76) Walker et al. (2012) Anti-Leukemic Activity of the CRM1 Inhibitor KPT-330 in Advanced CML and Ph+ ALL 54th ASH Annual Meeting Atlanta, GA, USA December 8–11, 2012.
- (77) Daelemans, D.; Afonina, E.; Nilsson, J.; Werner, G.; Kjems, J.; De Clercq, E.; Pavlakis, G. N.; Vandamme, A. M. A Synthetic HIV-1 Rev Inhibitor Interfering with the CRM1-Mediated Nuclear Export. *Proc. Natl. Acad. Sci. U. S. A.* **2002**, *99*, 14440–14445.
- (78) Ranganathan, P.; Yu, X.; Na, C.; Santhanam, R.; Shacham, S.; Kauffman, M.; et al. Preclinical activity of a novel CRM1 inhibitor in acute myeloid leukemia. *Blood* **2012**, *120*, 1765–1773.
- (79) Van Neck, T.; Pannecouque, C.; Vanstreels, E.; Stevens, M.; Dehaen, W.; Daelemans, D. Inhibition of the CRM1-Mediated Nucleocytoplasmic Transport by N-Azolylacrylates: Structure–Activity Relationship and Mechanism of Action. *Bioorg. Med. Chem.* **2008**, *16*, 9487–9497.
- (80) Sakakibara, K.; Saito, N.; Sato, T.; Suzuki, A.; Hasegawa, Y.; Friedman, J. M.; Kufe, D. W.; VonHoff, D. D.; Iwami, T.; Kawabe, T. CBS9106 Is a Novel Reversible Oral CRM1 Inhibitor with CRM1 Degrading Activity. *Blood* **2011**, *118*, 3922–3931.
- (81) Turner, J. G.; Dawson, J.; Emmons, M. F.; Cubitt, C. L.; Kauffman, M.; Shacham, S.; Hazlehurst, L. A.; Sullivan, D. M. CRM1 Inhibition Sensitizes Drug Resistant Human Myeloma Cells to Topoisomerase II and Proteasome Inhibitors Both in Vitro and Ex Vivo. *J. Cancer* **2013**, *4*, 614.
- (82) Monovich, L.; Koch, K. A.; Burgis, R.; Osimboni, E.; Mann, T.; Wall, D.; Gao, J.; Feng, Y.; Vega, R. B.; Turner, B. A.; Hood, D. B.; Law, A.; Papst, P. J.; Koditek, D.; Chapo, J. A.; Reid, B. G.; Melvin, L. S.; Pagratis, N. C.; McKinsey, T. A. Suppression of HDAC Nuclear Export and Cardiomyocyte Hypertrophy by Novel Irreversible Inhibitors of CRM1. *Biochim. Biophys. Acta, Gene Regul. Mech.* **2009**, *1789*, 422–431.
- (83) Gademann, K. Controlling Protein Transport by Small Molecules. *Curr. Drug Targets* **2011**, *12*, 1574–1580.
- (84) Azmi, A. S.; Aboukameel, A.; Bao, B.; Sarkar, F. H.; Philip, P. A.; Kauffman, M.; Shacham, S.; Mohammad, R. M. Selective Inhibitors of Nuclear Export Block Pancreatic Cancer Cell Proliferation and Reduce Tumor Growth in Mice. *Gastroenterology* **2013**, *144*, 447–456.
- (85) Bonazzi, S.; Eidam, O.; Güttinger, S.; Wach, J.-Y.; Zemp, I.; Kutay, U.; Gademann, K. Anguinomycins and Derivatives: Total Syntheses, Modeling, and Biological Evaluation of the Inhibition of Nucleocytoplasmic Transport. *J. Am. Chem. Soc.* **2010**, *132*, 1432–1442.
- (86) Kau, T. R.; Schroeder, F.; Ramaswamy, S.; Wojciechowski, C. L.; Zhao, J. J.; Roberts, T. M.; Clardy, J.; Sellers, W. R.; Silver, P. A. A Chemical Genetic Screen Identifies Inhibitors of Regulated Nuclear Export of a Forkhead Transcription Factor in PTEN-Deficient Tumor Cells. *Cancer Cell* **2003**, *4*, 463–476.
- (87) Wach, J.-Y.; Güttinger, S.; Kutay, U.; Gademann, K. The Cytotoxic Styryl Lactone Goniothalamin Is an Inhibitor of Nucleocytoplasmic Transport. *Bioorg. Med. Chem. Lett.* **2010**, *20*, 2843–2846.